

# ***In vivo*, high-resolution analysis of yeast and mammalian RNA–protein interactions, RNA structure, RNA splicing and ribozyme cleavage by use of terminal transferase-dependent PCR**

Hsiu-Hua Chen, Daniela Castanotto, Jeanne M. LeBon, John J. Rossi and Arthur D. Riggs\*

Departments of Biology and Molecular Biology, Beckman Research Institute of the City of Hope, Duarte, CA 91010, USA

Received August 23, 1999; Revised January 4, 2000; Accepted January 20, 2000

## **ABSTRACT**

**We have investigated the analysis of RNA by use of terminal transferase-dependent PCR (TDPCR), a procedure previously used for the analysis of DNA and chromatin [J.Komura and A.D.Riggs, *Nucleic Acids Res.*, 26, 1807–1811 (1998)]. When preceded by reverse transcription (RT), TDPCR provides an extremely sensitive, versatile, quantitative and nucleotide-level assay for detecting RNA lesions or structures that block primer extension during the RT step. The procedure is: (i) RT using a gene-specific oligonucleotide; (ii) ribo-tailing of the single-stranded cDNA product by use of terminal deoxynucleotidyl transferase; (iii) ligation of a DNA linker to the tailed cDNA by use of T4 DNA ligase; and (iv) PCR using a nested, gene-specific primer and a linker-specific primer. This procedure combines the versatility of a primer extension assay with nucleotide-level resolution, the specificity of nested primers and the sensitivity of PCR. Band patterns obtained are reproducible and quantifiable. We successfully used the technique for the study of yeast RNA structure, splicing intermediates and ribozyme cleavage. Also, *in vivo* footprint experiments, using mammalian cells and RNase T1, revealed the binding of iron-responsive element binding protein to iron responsive elements in the mRNAs of transferrin receptor and ferritin H-chain.**

## **INTRODUCTION**

Numerous methods, all dependent on reverse transcription (RT), have been devised for cDNA cloning and transcription start-site analysis in eukaryotic cells, including a method commonly called RACE for rapid amplification of cDNA ends (1,2). However, these and other methods (3) have been little used for *in vivo* analysis of eukaryotic RNA structure and protein–RNA interactions. This is in spite of the fact that all functions of RNA depend on specific secondary and tertiary structure determined by RNA–RNA or RNA–protein interactions, and these are likely to be quite different *in vivo*

than they are *in vitro*. Knowledge of *in vivo* RNA structure is also crucial for development of efficient antisense oligonucleotides and/or ribozymes, because secondary and tertiary structure renders many RNA regions inaccessible. Computer predictions are not yet adequate, so also for this purpose, sensitive, robust methods for *in vivo* RNA structure determination are needed.

An important improvement in the RACE procedure was made by Schmidt and Mueller (2) who introduced the use of ribo-tailing with terminal deoxynucleotidyl transferase (TdT) and then ligation to a DNA linker. Komura and Riggs (4) improved the linker, applied the technique to the study of DNA and chromatin structure, and named the procedure terminal transferase-dependent PCR (TDPCR) because of its relation to ligation-mediated PCR (LMPCR), a technique that has been much used for *in vivo* chromatin structure analysis and *in vivo* footprinting. There have now been >100 publications reporting use of LMPCR, which provides both qualitative and quantitative data with nucleotide-level resolution, nested primer specificity and PCR sensitivity (for reviews see 5,6). LMPCR cannot, however, be used for analysis of RNA because the procedure requires the use of T4 DNA ligase for addition of an oligo-deoxynucleotide linker to the 5' end of a DNA molecule.

Bertrand *et al.* (3) were the first to successfully adapt the linker-ligation concept for the analysis of RNA. They did this by adding an RNA oligonucleotide to the 5' end of RNA molecules by use of RNA ligase. The ligated RNA was then reverse transcribed into DNA, which was then used for PCR. This method, named RLPCR, has enough sensitivity to do LMPCR-type experiments in mammalian cells, and Bertrand and his colleagues (3,7) were able to detect *in vivo* protein–RNA footprints and ribozyme cleavage. Though this method seems to have good potential, there have been only a few reports of its successful use (3,7,8).

We report here that the application of the TDPCR approach to cDNA resulting from RT of mRNA leads to a powerful, versatile and extremely sensitive method for qualitative and quantitative RNA analysis, and it can be readily applied to yeast and mammalian cells. For study of prokaryotes, numerous less sensitive, and/or less specific, methods have been frequently used for the analysis of RNA structure (reviewed in 9). One common method involves treatment of cells, nuclei or isolated RNA with nucleases or chemicals, and then detection of RNA cleavage or adduct formation by use of RT for primer extension. Since RT–TDPCR, as described here,

\*To whom correspondence should be addressed. Tel: +1 626 301 8352; Fax: +1 626 358 7703; Email: ariggs@coh.org

is merely a sensitive, specific primer-extension assay, all such procedures previously used for prokaryotic cells should now be applicable to the study of RNA and RNA-protein interactions in eukaryotic cells. We find that RT-TDPCR is a robust, high-resolution, sensitive and quantitative method, suitable for analysis of yeast and mammalian RNA structure. The feasibility of the method is demonstrated by its use to detect splicing intermediates and ribozyme cleavage sites in yeast, as well as *in vivo* protein-RNA footprints in mammalian cells.

## MATERIALS AND METHODS

### Yeast strains, plasmid constructs, and RNA preparation

*Saccharomyces cerevisiae* JM43 (MATa, *leu2*, *ura3*, *trp1*, *his3*) was kindly provided by J. McEwen. The vectors transformed into this yeast strain are shown in Figure 2 and have been described previously (10,11). Briefly, pJYH7 contains a *S.cerevisiae* actin (ACT)-*lacZ* protein fusion that depends on splicing of the yeast ACT-1 intron for  $\beta$ -galactosidase expression. pJYH7MtRz was made by cloning a mutant, non-cleaving form of a *cis*-ribozyme (MtRz) into a unique *Sall* site, which is located at the ACT-*lacZ* fusion point (Fig. 2). pWC1Rz and pWC1MtRz were constructed by cloning a 192 nt *XhoI*-*Sall* fragment (nt positions 1648-1840) from exon II of the ACT gene into *Sall* digested pJYH7. The Rz and MtRz constructs were made by using two sets of complementary oligonucleotides: active ribozyme, 5'-TCGACCGCCGGCGAAACACCGGGTTCGCC-TGGTGTCTCGGACCTTCGGGTCCGACTGATGAGCCG-GCGG and 3'-GCGGCCGCTTTGTGGCCCAAGCGGACC-ACAGAGCCTGGAAGCCCAGGCTGACTACTCGGCCG-CCAGCT; mutant ribozyme, 5'-TCGACCGCCGGCGAAAC-ACCGGGTTCGCCCTGGTGTCTCGGACCTTCGGGTCCG-ACTAATGAGCCGGCGG and 3'-GCGGCCGCTTTGTGG-CCCAAGCGGACCACAGAGCCTGGAAGCCCAGGCTG-ATTACTCGGCCGCCAGCT.

Yeast transformants were grown in 10 ml of yeast synthetic minimal media (12) to an OD<sub>600</sub> of 0.8. The cultures were centrifuged at 1500 g for 5 min at 4°C, the supernatants were discarded and total RNA was prepared from the yeast pellets by a hot-phenol procedure (13,14).

### Enzymes, oligonucleotides and other reagents

**Magnetic beads.** Streptavidin-coated magnetic beads (Dynabeads M-280) were obtained from Dynal Inc. The beads are supplied by the manufacturer as a suspension containing  $6.7 \times 10^8$  Dynabeads/ml (10 mg/ml), dissolved in phosphate-buffered saline (PBS), pH 7.4, containing 0.1% BSA and 0.02% sodium azide. The capacity of the beads for oligonucleotides is ~200 pmol/mg, as stated by the manufacturer.

**Enzymes.** The following enzymes were used: AMV reverse transcriptase (20 U/ $\mu$ l; Life Science), Moloney M-MLV reverse transcriptase (200 U/ml; Gibco BRL); *C. therm.* polymerase (4 U/ $\mu$ l; Boehringer Mannheim), TdT (15 U/ $\mu$ l; Gibco BRL), T4 DNA ligase (3 U/ $\mu$ l; Promega), AmpliTaq polymerase (5 U/ $\mu$ l; Perkin Elmer) and T4 polynucleotide kinase (10 U/ $\mu$ l; New England Biolabs).

**Linker oligonucleotides.** As previously described (4,15), the TDPCR linker [linker gamma described by Komura and Riggs

(4)] is double-stranded DNA with a 3' CCC overhang. The lower strand is a 24mer with an aminopentyl blocking group at the 3' end [5'-AATTCAGATCTCCCGGGTCAACCGC-NH<sub>2</sub>, see (4)]. This oligonucleotide must be 5' phosphorylated before use. The upper strand is a 27mer (5'-GCGGTGAC-CCGGGAGATCTGAATTCCC-3'). To prepare double-stranded linker, an equimolar amount of upper strand was added directly to the post-kinased lower strand in kinase buffer. The mixture was heated to 95°C and cooled gradually to room temperature. The linker was stored at -20°C. Before use it was thawed and kept on ice. The oligonucleotide used for the linker primer is a 25mer (LP25), the same linker primer as conventionally used for LMPCR (5,15). The sequence of LP25 is the same as the upper strand of the TDPCR linker shown above except 2 nt shorter, i.e. only one C at the 3' end.

**Gene specific primers.** The sequences of primers used in this study are given in the figure legends. Usually, three nested primers should be used for TDPCR or RT-TDPCR, but in favorable cases only two may be needed, such as is the case for the yeast experiments shown here. Primer 1 is a 5'-biotinylated primer used for first strand synthesis by RT (Fig. 1). Primer 2 is a nested primer used for the PCR and primer 3 is used for the final labeling step. The P1 primers for AMV and M-MLV RTs were designed to be specific at 42°C. For experiments using *C. therm.*, P1 primer had a  $T_m$  of 70°C.  $T_m$  was calculated using the Oligo™ 4.0 computer program (National Biosciences, Plymouth, MN) with default settings (50 mM salt and 250 pM oligonucleotide concentrations). P2, the nested gene-specific primer, was designed to have a  $T_m$  within 5°C of LP25, the common linker primer, which has a calculated  $T_m$  of 63°C. The annealing temperature in the PCR step was chosen to be at the  $T_m$  of the gene-specific primer. Primer 3 was designed to have a  $T_m$  greater than primer 2, so that competition during direct labeling would be minimized.

### RNase T1 treatment (*in vivo* footprinting) of Hep G2 cells

Human Hep G2 cells were grown, treated and used for RNA preparation as described by Bertrand *et al.* (3). In brief, cells were first grown in 10-cm plates in DMEM medium plus 10% calf serum to near 80% confluency. The cells were washed with 1× PBS and then incubated overnight in serum-free DMEM in the presence of either 100  $\mu$ M hemin or desferrioxamine. The cells were trypsinized, washed once with 1× PBS, resuspended in 1× PBS and counted. For RNase T1 treatment,  $1 \times 10^6$  cells in 100  $\mu$ l of ice-cold physiological buffer (3) were mixed with 100  $\mu$ l of ice-cold physiological buffer containing 0.4% Nonidet P-40 and various amounts (0-200 U) of RNase T1. After incubation at 4°C for 3 min, nuclei were removed by centrifugation and cytosolic RNA was prepared by SDS/phenol extraction as described (3).

### The RT-TDPCR procedure

**First strand synthesis for yeast RNA using AMV RT.** An annealing mixture was made by adding 5  $\mu$ g of total yeast RNA to 0.6-1 pmol of biotinylated primer 1 (see figure legends for primer sequences) in 1× RT buffer (50 mM Tris, pH 8.6 at 25°C, 60 mM NaCl, 10 mM DTT) in a total volume of 10  $\mu$ l. The mixture was heated at 80-85°C for 3-5 min in a heat block, allowed to cool slowly to room temperature, spun briefly and placed on ice. While on ice, 2  $\mu$ l of 36 mM

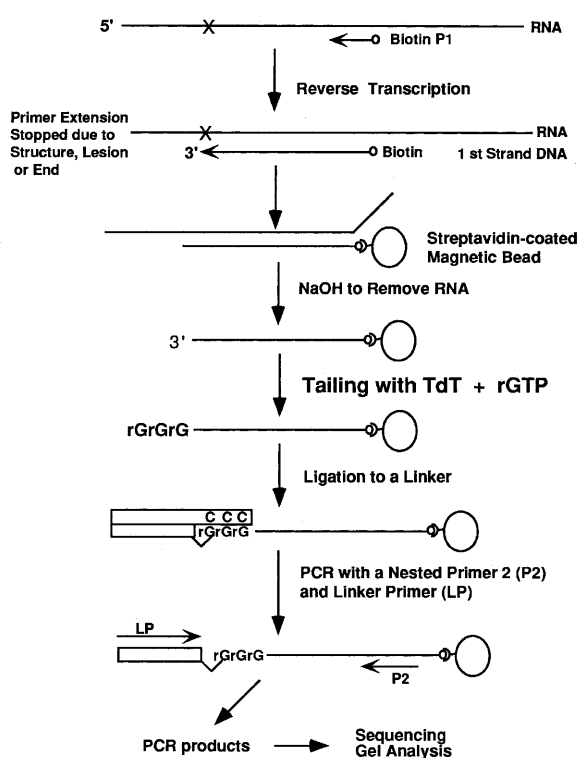


**Figure 1.** Schematic outline of the RT-TDPCR procedure. RNA is reverse transcribed using a biotin-labeled, gene-specific primer (P1) and the newly synthesized cDNA strand is ribo-tailed using TdT and riboGTP. An oligonucleotide linker with a blocked 3'-terminus is then ligated to the tailed, 3' end of the cDNA strand. The cDNA molecules, now having a defined sequence on both the 5' and 3' ends, are PCR amplified using a nested gene-specific primer (P2) and a linker-specific primer (LP). The amplified DNA fragments are labeled, usually by using a third gene-specific primer (P3), separated by use of a DNA sequencing gel and visualized by autoradiography or phosphorimaging.

Mg(OAc)<sub>2</sub> in 1× RT buffer was added. Three microliters of the annealed sample was transferred to a new tube. Two microliters of a freshly prepared RTase/dNTP mix [dilute AMV RTase to 4–5 U/μl with 1× RT buffer plus 6 mM Mg(OAc)<sub>2</sub> and add to an equal volume of 5× dNTP (1.875 mM each) in the same buffer] was added and the reaction was incubated at 42°C for 45 min.

**First strand synthesis for mammalian cells using Moloney MuLV RT.** A pre-RT mixture (10 μl) was made containing 250 ng of total Hep G2 RNA, 1 pmol of biotinylated primer 1 in 1× PCR buffer II (10 mM Tris, pH 8.3, 50 mM KCl) containing 5 mM MgCl<sub>2</sub>, 2.5 mM dNTP and 6 U RNasin (Promega). The mixture was overlaid with mineral oil, heated to 85°C for 5 min in a heat block, allowed to cool slowly to 42°C and then put at room temperature. An RT reaction mixture (10 μl) was added which contained 1× PCR buffer II, 5 mM MgCl<sub>2</sub>, 10 U of RNasin and 70 U of Moloney M-LV RT. The reaction was mixed, spun briefly, incubated at 42°C for 45 min, denatured at 95°C for 5 min and then placed on ice.

**First strand synthesis for mammalian cells using *C. therm.* polymerase.** An RT reaction mixture (20 μl) was made according to manufacturer's instructions for *C. therm.*

polymerase (Boehringer Mannheim). The reaction contained 4 μl of 5× RT buffer supplied by the manufacturer (with 25 mM MgCl<sub>2</sub> and 10% DMSO), 1 μl of 100 mM DTT, 0.64 μl of 25 mM dNTP, 0.6 μl of 100% DMSO, 20 pmol of biotinylated primer 1, 250 ng of total Hep G2 RNA and 1.5 μl of *C. therm.* polymerase (6 U). The mixture was overlaid with mineral oil, incubated at 70°C for 30 min and then placed on ice.

**Extension product capture and enrichment using magnetic beads.** Usually 200 μl of streptavidin-coated beads, enough for 10 samples, were washed as a batch in a 1.5 ml eppendorf tube 2–3 times with 400 μl of 2× B&W buffer (10 mM Tris-HCl, pH 7.5, 1 mM EDTA, 2 M NaCl). A magnetic particle concentrator was used to separate the beads. The washed beads were suspended in 200 μl of 2× B&W buffer. Twenty microliters of washed bead suspension was added to 5–20 μl of the cDNA product from the previous step and the mixture was rotated or gently agitated at room temperature for 15–60 min (longer incubation for longer products, following the suggestion from the manufacturer). The supernatant was removed and the beads washed once with 60 μl of 2× B&W buffer. Fifty microliters of 0.15 M NaOH then was added and the suspension was incubated at 37°C for 5–10 min. This step removes the mRNA template but leaves the DNA on the beads. The supernatant was removed and the beads were washed once more with 50 μl of 0.15 M NaOH. The beads were neutralized by washing twice with 100 μl TE, pH 7.5 (10 mM Tris-HCl, 1 mM EDTA) and suspending them in 10 μl of 0.1× TE, pH 7.5.

**Ribo-tailing of cDNA on the beads using TdT.** To the neutralized beads was added 10 μl of a TdT mixture containing 10 U of TdT and 4 mM riboGTP in the 2× TdT buffer supplied by the manufacturer. The reaction mixture was incubated at 37°C for 15 min. The supernatant was removed and the beads were washed twice with 100 μl TE, pH 7.5, and then suspended in 15 μl of 0.1× TE, pH 7.5.

**Ligation of the riboG-tailed DNA to a double-stranded DNA linker.** To the bead suspension was added 15 μl of 2× ligation mix consisting of 7.95 μl of H<sub>2</sub>O, 1.5 μl of 1 M Tris-HCl, pH 7.5, 0.3 μl of 1 M MgCl<sub>2</sub>, 0.3 μl of 1 M DTT, 0.3 μl of 100 mM ATP, 0.15 μl of 10 mg/ml BSA, 3 μl of TDPCR linker and 1.5 μl T4 DNA ligase. The reaction was incubated overnight in a 17°C water bath. The beads were washed twice with 100 μl TE, pH 8.0 and resuspended in 30 μl 0.1× TE, pH 8.0.

**PCR.** Usually 10 μl (out of 30 μl total) of the washed beads from the step above was transferred to a new tube. However, much less can often be used. With yeast RNA, for example, even 1 μl of beads gave a good signal. To the beads was added 40 μl of PCR mix consisting of 27.4 μl H<sub>2</sub>O, 10 μl of 5× *Taq* buffer [200 mM NaCl, 50 mM Tris-HCl, pH 8.9, 0.05% (w/v) gelatin], 0.1 μl of 1 M MgCl<sub>2</sub>, 0.5 μl of 25 mM dNTP mix, 0.5 μl of 20 μM primer 2, 0.5 μl of 20 μM LP25 (the linker primer) and 1 μl of *AmpliTaq* (5 U/μl). The reaction was overlaid with 50 μl mineral oil and 20 thermocycles were done (45 s at 95°C, 2 min at 63°C, or a temperature close to the *T<sub>m</sub>* of primer 2, and 3 min at 74°C). The PCR product was kept at 4°C until used for labeling and/or electrophoresis. Freezing was avoided so that *AmpliTaq* will remain adequately active for the subsequent labeling step. For reactions containing

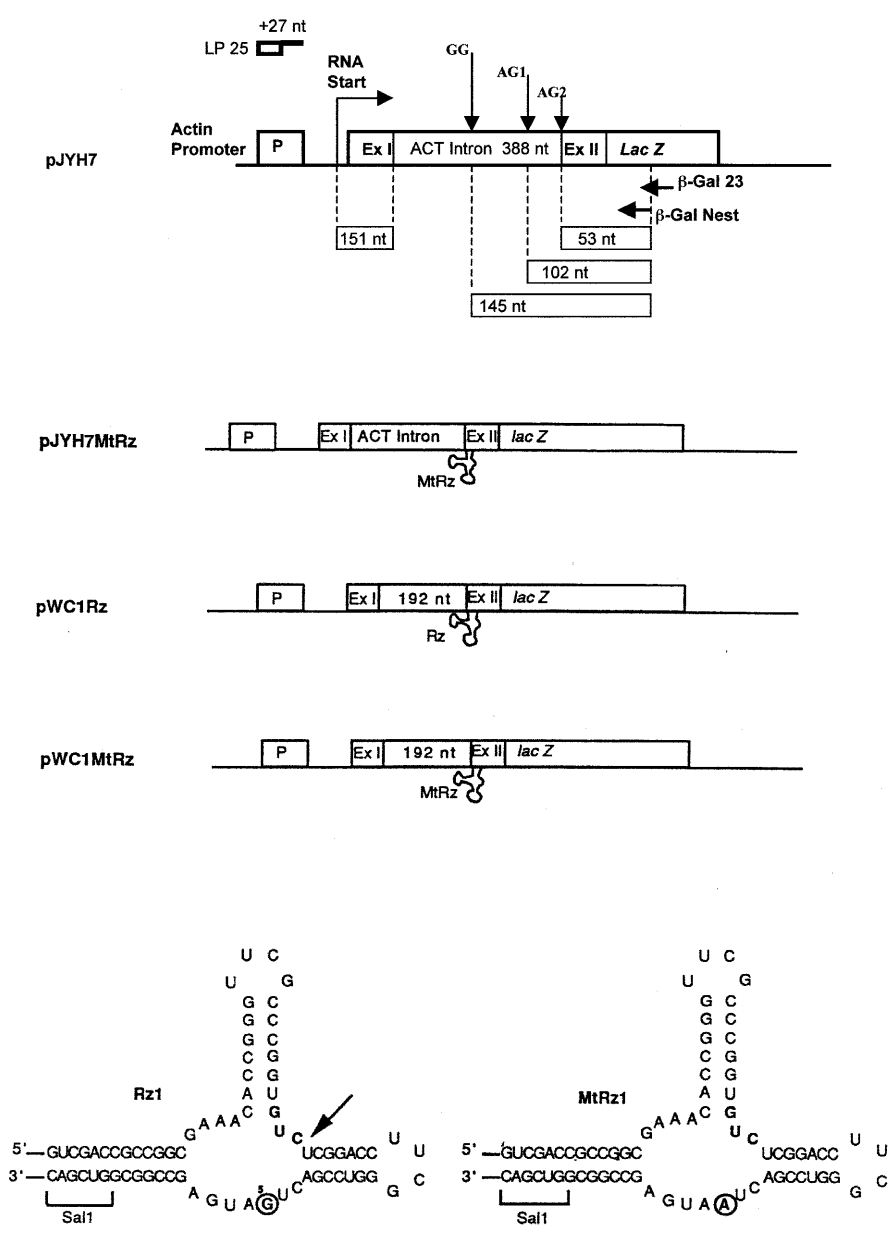


**Figure 2.** Yeast plasmid constructs and ribozymes. Ex I and Ex II depict exon I and II, respectively, of the yeast actin gene. For pJYH7, the size of the RNA transcript components and the position of the GG, AG1 and AG2 splice sites in the actin intron are indicated. For pWC1Rz, the element labeled 192 nt is a yeast exon II fragment that does not have a splice site. The location of the ribozyme, either Rz or MtRz, at the junction of the 192 nt and exon II fragments is shown. Also shown above the constructs is the 25 nt linker, as a reminder that this linker becomes a component of each RT-TDPCR fragment and must be taken into account when calculating the size of expected fragments. The last gene-specific primer used, in these cases  $\beta$ -Gal Nest, also becomes a component of each TDPCR fragment. These ribozymes and constructs have been described previously (11). The ribozymes used in this study, Rz and MtRz, differ only at one position in the active site, as indicated by the circled bases. The arrow indicates the site at which cleavage will occur after transcription.

betaine, the PCR was done as previously described, with the exception that 15  $\mu$ l of 5 M betaine was included in the reaction mixture to make the final concentration 1.5 M.

**Direct labeling.** Ten microliters of the PCR product was transferred to a new tube and 1  $\mu$ l of 5'  $^{32}$ P-labeled primer 3 (~1 pmol) was added. The reaction was overlaid with 10  $\mu$ l of mineral oil and 3–6 thermocycles were done (45 s at 95°C, 2 min at 65°C and 3 min at 72°C).

**Gel electrophoresis.** Five microliters of labeled sample was mixed with 5  $\mu$ l of loading dye. This sample was heated at 95°C for 2 min just before loading 1–10  $\mu$ l on a 6–8% standard denaturing DNA sequencing gel. After electrophoresis the separated fragments of the gel ladder were visualized by autoradiography or by use of a phosphorimager. An alternative to direct labeling is transfer of the unlabeled gel-separated fragments to a membrane and then visualization by hybridization with a labeled probe. This procedure, which is commonly used



able to detect the remaining uncleaved transcript even though the intensity of the band representing full-length transcripts is only 4% of that seen for the mutant ribozyme construct. The identity of the 111 nt cleavage product was confirmed by isolating the band from the gel and determining its sequence. As shown in Figure 4, cleavage was exactly at the expected site; plasmid sequence is followed by the ribozyme sequence to the cleavage site, the guanosines added by TdT and then the sequence of the linker. This is a generally useful feature of RT-TDPCR; any band can be isolated from the gel and its sequence determined by sequencing either directly or after cloning.

### Structurally determined pause sites

In addition to a strong 492 nt band representing extension to the 5' end of the mRNA, the lanes with both the active and inactive ribozyme have a cluster of bands centered at 78 nt. This band cluster is at the site of insertion of the ribozyme and probably results from structure-induced pausing of RT during primer extension. This is to be expected, since previous work has shown ribozyme structure to cause pausing of AMV RT (18). A cluster of bands is seen, not a single band, because of variable addition of Gs by TdT.

The bands centered at 90 nt, which are present in pWC1Rz but not in pWC1MtRz, are of interest because they demonstrate that RT-TDPCR is detecting subtle RNA structural changes that are occurring after ribozyme cleavage. A pause site at 90 nt is consistent with structural predictions based on nucleotide base interactions detected by NMR in the cleaved ribozyme after cleavage (19,20).

### Alternative pre-mRNA splicing

Transcripts of pJYH7 and pJYH7MtRz (Fig. 2) are known to undergo alternative pre-mRNA splicing (21). We used pJYH7 and pJYH7MtRz constructs to see if alternative splice products could be detected by RT-TDPCR as well as structural features of the RNA transcripts that may be important for the splicing reaction. pJYH7 and pJYH7MtRz contain three different 3' splice sites GG, AG1 and AG2 (21) which are shown in Figure 2. An exon II primer that has its 5' end located 53 nt downstream of the last 3' splice site should generate RT-TDPCR products of 231 (153+53+27), 280 (151+102+27) and 323 (151+145+27) nt with pJYH7, whereas pJYH7MtRz should generate 349 and 392 nt products. (The 27 nt is added because the RT-TDPCR products each will have an additional 27 nt due to the LP25 linker.) The difference in mRNA sizes between pJYH7 and pJYH7MtRz is due to the presence of 69 nt from the mutant ribozyme in exon 2 of the pJYH7MtRz spliced products. pJYH7MtRz should generate only two spliced products, since the insertion of the ribozyme in exon 2 completely blocks splicing at the last 3' splice site (18). The sizes of the RT-TDPCR products from the unspliced pre-mRNA transcripts are 619 nt for pJYH7 and 688 nt for pJYH7MtRz.

Figure 3 shows that the expected RT-TDPCR products from unspliced and spliced mRNAs are seen, as well as the ribozyme cleavage products. For example, since the insertion of the mutant ribozyme blocks splicing at the 3'-most splice site AG2, we would expect branch point accumulation within this transcript. The RT-TDPCR analysis of this construct is able to detect a 271 nt fragment, which corresponds to an RT stop at the branch site of this pre-mRNA (Fig. 3, lanes 3 and 7).

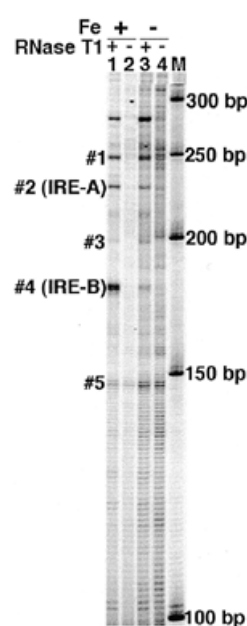


**Figure 5.** *In vivo* RNase T1 footprinting of human transferrin receptor mRNA by RT-TDPCR. Hepatoma cells (38) were treated overnight with either 100  $\mu$ M hemin (+Fe, lanes 1 and 2) or desferrioxamine (-Fe, lanes 3 and 4) added to the medium. Cells were treated with 200 U of RNase T1 (lanes 1 and 3) or no RNase T1 (lanes 2 and 4) according to the procedure in Materials and Methods (3). Cytosolic mRNA was isolated and used for TDPCR. The primer set used was: primer 1, 5'-biotin-CTAAATCTTAGCTTCAAC; primer 2, 5'-AACTT-TATTCAATTACATTTGGCTG and primer 3, 5'-ATTCAATTACATTTGGCTGACGGCTG. Lane M shows a 50 bp DNA ladder. The iron-responsive elements IRE-A and IRE-B are indicated, as are the bands (#1-#5) used for quantitative analysis (Fig. 6).

As expected, the 78 nt product that is a result of pausing caused by the presence of the *cis*-ribozyme in the RNA transcripts is absent in pJYH7 (Fig. 3, lanes 4 and 8).

### RNase T1 footprinting to detect protein-RNA interactions in mammalian cells

To demonstrate that RT-TDPCR can be used to study *in vivo* protein-RNA interactions as well as RNA structure in mammalian cells, we first chose the transferrin receptor system. This is the same system previously used by Bertrand *et al.* (3) to demonstrate that RLPCR can be used for *in vivo* RNA footprinting by RNase T1 treatment of permeabilized cells. In the absence of iron, iron-responsive-element binding protein (IRE-BP) binds RNA elements (IREs) which are found in several mRNAs and thought to fold into a stem-loop structure (see Fig. 8). Several IREs of various binding affinities are located in the 3'-UTR of transferrin receptor mRNA (22). In the absence of iron, IRE-BP binds to transferrin receptor mRNA and inhibits its degradation. Iron inhibits the binding of IRE-BP, increases mRNA degradation and thus reduces the level of transferrin receptor protein.

RNase T1 is specific for Gs in single-stranded RNA (9). As was done by Bertrand *et al.* (3), we treated human hepatoma cells (Hep G2) with RNase T1 and purified total cytosolic RNA. We then did RT-TDPCR using primers specific for the 3'-UTR of the transferrin receptor mRNA. Figure 5 shows that RNA from cells treated with RNase T1 show numerous bands (Fig. 5, lanes 1 and 3) that are not seen in mock treated cells

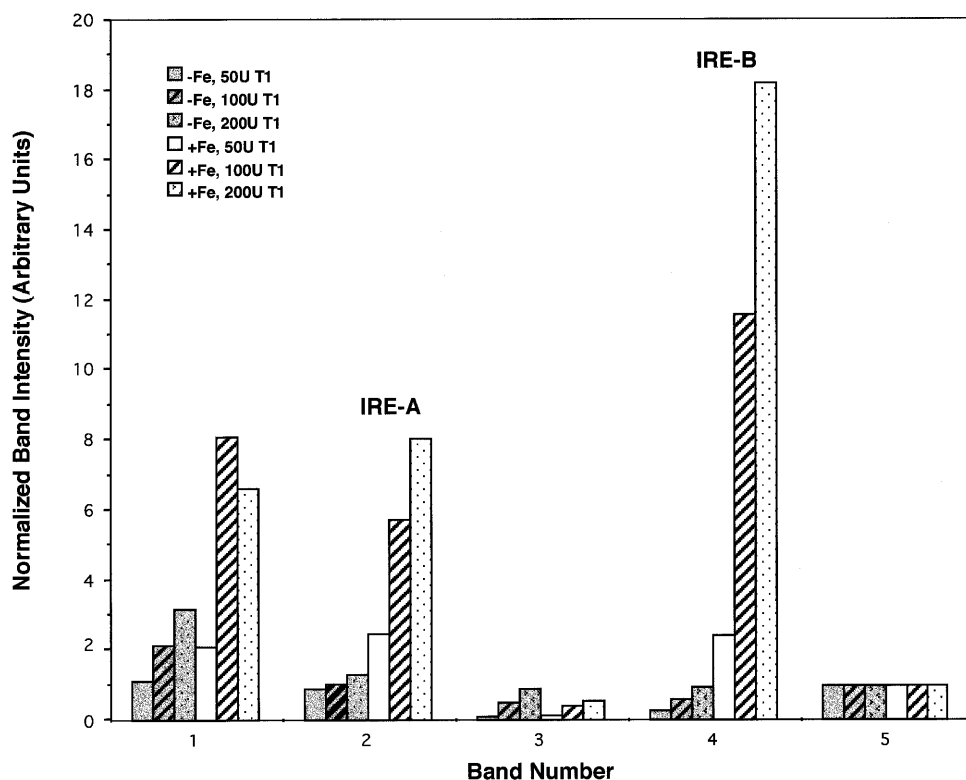


**Figure 6.** Dose dependence and quantitative analysis of transferrin receptor mRNA footprinting. Integrated band intensities were determined for the bands marked #1 to #5 in Figure 5 and for experiments not shown. To aid correction for loading and other variations, the bands were normalized to band #5, which is a band that is independent of RNase T1. As indicated in the figure, unshaded bars are from cells treated with hemin (+Fe) and shaded bars are cells treated with desferrioxamine (–Fe). The various concentrations of RNase T1 (0–200 U) used to treat the cells are indicated by different patterns, as shown in the figure.

(Fig. 5, lanes 2 and 4). A site of strong RNase T1 cleavage is seen at the position expected for IRE-B (Fig. 5, band #4) for cells grown in the presence of hemin (+Fe; Fig. 5, lanes 1 and 3), but this band is much less for cells grown in the presence of the iron chelator desferrioxamine (–Fe; Fig. 5, lane 3). IRE-B is known to be a high-affinity site for IRE-BP (22). At IRE-A, a second, lower affinity site previously identified by *in vitro* studies (22), the change induced by iron is not so obviously dramatic; but when a dose–response curve is done and corrections made for loading, there is a similar response to iron as seen for IRE-B (Fig. 6). These results obtained using RT–TDPCR thus confirm and extend the earlier *in vitro* (22) and *in vivo* (3) studies.

The level of ferritin protein is also controlled by iron, but in contrast to transferrin receptor, it is upregulated by iron, rather than downregulated. *In vivo* footprinting studies have not previously been reported, but previous studies led to identification of an IRE near the 5′ end of the ferritin H-chain message (23). In the absence of iron, the IRE-binding protein is thought to bind at this IRE and inhibit translation. In our initial studies on ferritin H-chain mRNA, we found that full-length RT–TDPCR fragments were difficult to obtain. This problem was solved by using *C. therm.* polymerase, a thermostable RT, and including betaine in the PCR reaction. Though the use of *C. therm.* gives a somewhat lower background (data not shown), the presence of betaine during PCR gave the main improvement (Fig. 7). Apparently, the sequence at the 5′ end of ferritin is difficult for *Taq* polymerase to amplify. Betaine is known to aid PCR

amplification of difficult sequences (24). Figure 7 thus shows that excellent results can be obtained even for a difficult sequence that is 73% G+C. Note the reproducibility between lanes, even for low intensity bands. Importantly, one sees a dramatic effect of iron on RNase T1 susceptibility at the IRE, which is known to be located between –151 and –186, ~46 nt from the transcription start site (23). As evidenced by little change in the RNase T1 cleavage pattern, the overall structure of the 5′ region analyzed was not changed by iron. There are 22 Gs located within the first 80 bp of the ferritin H-chain mRNA, and all except for those in the IRE react weakly with RNase T1. These results are consistent with the structure of the IRE loop and stem predicted by the mfold program (25,26) and shown in Figure 8. *In vitro* NMR studies using synthetic RNA have detected interactions between G<sub>47</sub> and C<sub>43</sub> in the hexaloop (using the base numbering shown in Fig. 8), and also between U<sub>35</sub> and G<sub>55</sub> in the internal loop/bulge (27,28). Our studies do not add information at this level of detail, but do provide evidence that the structure of ferritin IRE *in vivo* is quite similar to that *in vitro*.

#### Reproducibility and quantitation

Previous studies established that LMPCR and TDPCR can be used for both qualitative and quantitative analysis of DNA (4,29). The pattern of relative band intensities is quite reproducible. The method is quantitative and rather robust in this aspect. We find that RT–TDPCR is similarly quantitative. Two separate experiments are shown in Figure 3. The RNAs were prepared

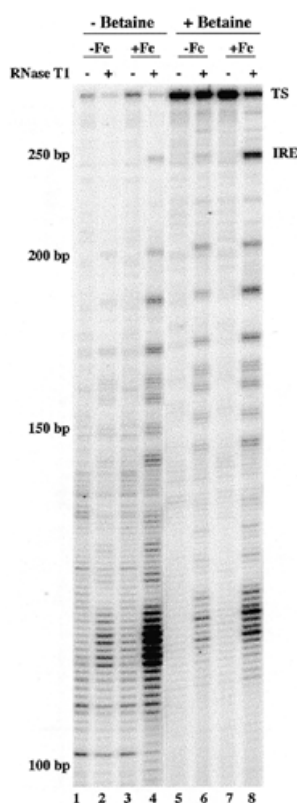


**Figure 7.** RNase T1 footprinting of ferritin H-chain mRNA by RT-TDPCR. Hepatoma cells were treated as in Figure 5 with either 100  $\mu$ M desferrioxamine (-Fe, lanes 1, 2, 5 and 6) or 100  $\mu$ M hemin (+Fe, lanes 3, 4, 7 and 8). Cytosolic mRNA was isolated after RNase T1 treatments (0 U, lanes 1, 3, 5 and 7, or 100 U, lanes 2, 4, 6 and 8). The primer set used was: primer 1, 5'-biotin-GCTCCAGGTGATCTGGCGGTTGATG; primer 2, 5'-CGGTTGATGGCGGCCTCTGAGTC and primer 3, 5'-GGCGGCCTCTGAGTCCTGGTGGTAG. The PCR step was done either with (lanes 5-8) or without (lanes 1-4) 1.5 M betaine. TS denotes the transcription start site and IRE denotes the iron response element.

at different times and one sample was stored for months before RT-TDPCR assay. Inspection of the patterns shows excellent reproducibility. Even minor bands are at the same relative intensities in the two experiments. Moreover, the relative ratios of utilization of the various 3' splice sites detected by RT-TDPCR are similar to results obtained in earlier studies that utilized PCR but only visualized spliced transcripts (21). Good reproducibility is also seen for mammalian studies. The relative intensity of even faint bands, including those in the lanes without RNase T1 (Fig. 7, compare lanes 5 and 7), is quite reproducible. Thus TdT tailing seems to be rather robust, as are other steps in the procedure. These studies with RNA thus show excellent reproducibility, as did the previous studies using TDPCR to study DNA (4).

The change in RNase T1 susceptibility in response to iron at the IRE-B element in transferrin receptor mRNA is obvious by visual inspection of Figure 5. However, quantitative analysis can be even more informative, as shown in Figure 6. Digitized data, obtained by use of a phosphorimager, were used to calculate integrated band intensities for the bands labeled #1-#5 in Figure 5. To correct for variable gel loading (e.g. lane 2 of Fig. 5

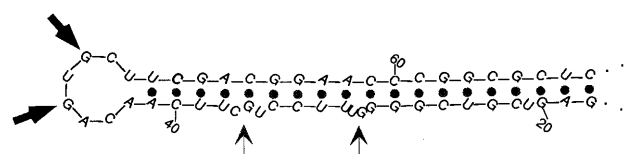


**Figure 8.** Possible structure for the ferritin H-chain IRE. The mfold program (25,26) (<http://www.ibc.wustl.edu/~zucker/mfold/>) was used with default parameters to model the first 300 bp of ferritin H-chain mRNA (accession no. L20941). The predicted stem-loop structure for IRE region is shown. Sites of strong RNase T1 cleavage in the loop of the IRE are shown by thick arrows. Thin arrows show sites of minor cleavage in the stem. The nucleotide positions are relative to the transcription start.

has weaker bands than lane 4), the data were normalized using a band showing no RNase T1 dose dependence. Band #5 is present in all lanes and shows no dose response to RNase T1 (Fig. 5 and data not shown). This band, which likely comes from pausing due to RNA structure during primer extension, was used to normalize, and Figure 6 shows the results obtained. Both the dose response to RNase T1 and the changes in susceptibility in the presence of iron are clearly seen. For example, the susceptibility of IRE-B is increased 18-fold by iron.

## DISCUSSION

RNA structure and protein-RNA interactions (9,30) have been studied greatly because they are crucial for RNA function. However, most of the techniques used, including those that depend on primer extension, work well for prokaryotes but have seen limited use for mammalian cells because of detection and specificity limitations. For example, primer extension reactions to determine transcription start sites for mammalian mRNA require as much as 60  $\mu$ g of RNA and long exposure times (31-33). Detection of low abundance RNA lesions, such as those expected due to splicing intermediates, ribozyme cleavage and protein-RNA footprinting agents, cannot be done by primer extension without some additional signal amplification technique. Bertrand *et al.* (3) developed the first technique with sensitivity adequate for detection of *in vivo* footprints (3) and ribozyme cleavage (7). Their technique, which they named RLPCR, only detects 5'-phosphorylated RNA ends to which an RNA linker has been ligated before the primer extension reaction. RNA structure or lesions that stop primer extension are not detected. This may often be an advantage, since, theoretically, the background should be low and due only to RNA strand breaks. However, in their experiments significant background was seen in RNA from cells not treated with RNase T1; presumably this was due to endogenous RNase cleavage before or during RNA preparation, kination and ligation (3). We find that RT-TDPCR analysis of RNA from cells not treated with RNase T1 can have a relatively low background (Fig. 7, lanes 5 and 7).

TDPCR for DNA studies (4) and, as we report here, RT-TDPCR for RNA studies each retains most of the advantages of LMPCR, a technique that has been much used for the study of *in vivo* protein-DNA interactions because it gives PCR sensitivity, nested primer specificity and nucleotide-level resolution (5,15,29,34). Usually LMPCR needs for detection only about 100 template molecules at a specific size for each band seen in the



gel ladder. TDPCR can be several-fold more sensitive than LMPCR for DNA (4), but for RNA, sensitivity is similar to LMPCR. RT-TDPCR should thus need for detection only a few hundred RNA molecules. Experiments reported here were not directed at determining the ultimate sensitivity of the method, but we have been able to determine transcription initiation sites using as little as 6 ng of total RNA (data not shown), and, as reported in a companion paper, even single cells can be analyzed by using a variation of the method (35).

In addition to being extremely sensitive, both LMPCR and TDPCR have proven to be quite quantitative; being capable of detecting reproducibly even 2-fold differences (29), as long as the primers and active enzyme are in vast excess, which is the case for at least the first 20 PCR cycles. The ratio of nearby bands is very reproducible, so changes in the ratio of bands within the same lane are diagnostic of changes in DNA structure or protein-DNA interactions. This feature of TDPCR should be the same for RT-TDPCR, and experiments reported here have confirmed this expectation. In fact, the primary finding of this paper is that RT-TDPCR can be used to derive reproducible, quantitative information from the less than full-length cDNA transcripts that result from RT pausing or stopping due to intrinsic RNA structure or experimentally introduced breaks or lesions.

We have successfully used RT-TDPCR to (i) detect *cis*-ribozyme cleavage of mRNA in transformed yeast cells (Fig. 3), (ii) confirm the location of a transcription start site in yeast (Fig. 3) and mammalian cells [Ferritin H-chain, Fig. 7; Xist, data not shown; Snrpn, Buettner *et al.* (35)], (iii) detect mRNA splicing intermediates (Fig. 3), (iv) detect protein-RNA interactions by *in vivo* RNase T1 footprinting (Figs 5 and 7) and (v) gain information on RNA structure, as evidenced by pause sites (Fig. 3) and susceptibility to RNase T1 (Figs 5-7). We expect that any agent that cleaves or modifies RNA and blocks the progression of primer extension can be used for analysis. This category includes a large number of agents, such as alkylating chemicals, UV and psoralen that have been used for structure determination of prokaryotic RNA (9,30,36). Another potentially important application of RT-TDPCR is for the detection of 3' cleavage products produced by *in vivo* ribozyme cleavage. In many cell types, products are quickly degraded and cannot be detected by RNase protection or primer extension analyses (37).

## ACKNOWLEDGEMENTS

This work was supported by NIH grants GM50575 to A.D.R. and AI29329 to J.J.R.

## REFERENCES

1. Frohman, M.A. (1993) *Methods Enzymol.*, **218**, 340-356.
2. Schmidt, W.M. and Mueller, M.W. (1996) *Nucleic Acids Res.*, **24**, 1789-1791.
3. Bertrand, E., Fromont-Racine, M., Pictet, R. and Grange, T. (1993) *Proc. Natl Acad. Sci. USA*, **90**, 3496-3500.
4. Komura, J. and Riggs, A.D. (1998) *Nucleic Acids Res.*, **26**, 1807-1811.
5. Hershkovitz, M. and Riggs, A.D. (1997) *Methods*, **11**, 253-263.
6. Riggs, A.D. and Pfeifer, G.P. (1997) In Cartwright, I.L. (ed.), *In Vivo Footprinting*, Vol. 21. JAI Press, Greenwich, CT, pp. 47-72.
7. Bertrand, E., Fromont-Racine, M., Pictet, R. and Grange, T. (1997) *Methods Mol. Biol.*, **74**, 311-323.
8. Giles, R.V., Spiller, D.G. and Tidd, D.M. (1995) *Antisense Res. Dev.*, **5**, 23-31.
9. Ehresmann, C., Baudin, F., Mougel, M., Romby, P., Ebel, J.P. and Ehresmann, B. (1987) *Nucleic Acids Res.*, **15**, 9109-9128.
10. Castanotto, D., Chow, W.A., Li, H. and Rossi, J.J. (1998) *Antisense Nucleic Acid Drug Dev.*, **8**, 499-506.
11. Castanotto, D., Li, H., Chow, W., Rossi, J.J. and Deshler, J.O. (1998) *Antisense Nucleic Acid Drug Dev.*, **8**, 1-13.
12. Sherman, F., Fink, G.R. and Hicks, J.G. (1986) *Methods in Yeast Genetics*. Cold Spring Harbor Laboratory Press, Cold Spring Harbor, New York.
13. Domdey, H., Apostol, B., Lin, R.J., Newman, A., Brody, E. and Abelson, J. (1984) *Cell*, **39**, 611-621.
14. Lin, R.-J., Kim, D.-H., Castanotto, D., Westaway, S. and Rossi, J.J. (1996) In Kreig, P.A. (ed.), *A Laboratory Guide to RNA: Isolation, Analysis, and Synthesis*. Wiley-Liss, New York, NY, pp. 43-50.
15. Pfeifer, G.P., Chen, H.H., Komura, J. and Riggs, A.D. (1999) *Methods Enzymol.*, **304**, 548-571.
16. Denissenko, M.F., Koudriakova, T.B., Smith, L., O'Connor, T.R., Riggs, A.D. and Pfeifer, G.P. (1998) *Oncogene*, **17**, 3007-3014.
17. Ruffner, D.E., Stormo, G.D. and Uhlenbeck, O.C. (1990) *Biochemistry*, **29**, 10695-10702.
18. Lin, J. and Rossi, J.J. (1996) *RNA*, **2**, 835-848.
19. Simorre, J.P., Legault, P., Hangar, A.B., Michiels, P. and Pardi, A. (1997) *Biochemistry*, **36**, 518-525.
20. Murray, J.B., Terwey, D.P., Maloney, L., Karpeisky, A., Usman, N., Beigelman, L. and Scott, W.G. (1998) *Cell*, **92**, 665-673.
21. Deshler, J.O. and Rossi, J.J. (1991) *Genes Dev.*, **5**, 1252-1263.
22. Koeller, J.B., Casey, J.L., Hentze, M.W., Gerhardt, E.M., Chan, L.N., Klausner, R.D. and Harford, J.B. (1989) *Proc. Natl Acad. Sci. USA*, **86**, 3574-3578.
23. Hentze, M.W., Caughman, S.W., Rouault, T.A., Barriocanal, J.G., Dancis, A., Harford, J.B. and Klausner, R.D. (1987) *Science*, **238**, 1570-1573.
24. Henke, W., Herdel, K., Jung, K., Schnorr, D. and Loening, S.A. (1997) *Nucleic Acids Res.*, **25**, 3957-3958.
25. Mathews, D.H., Sabina, J., Zuker, M. and Turner, D.H. (1999) *J. Mol. Biol.*, **288**, 911-940.
26. Zuker, M., Mathews, D.H. and Turner, D.H. (1999) In Barciszewski, J. and Clark, B.C.F. (eds), *RNA Biochemistry and Biotechnology*. Kluwer Academic, Dordrecht, The Netherlands.
27. Gdaniec, Z., Sierzputowska-Gracz, H. and Theil, E.C. (1998) *Biochemistry*, **37**, 1505-1512.
28. Address, K.J., Babilion, J.P., Klausner, R.D., Rouault, T.A. and Pardi, A. (1997) *J. Mol. Biol.*, **274**, 72-83.
29. Pfeifer, G.P., Tanguay, R.L., Steigerwald, S.D. and Riggs, A.D. (1990) *Genes Dev.*, **4**, 1277-1287.
30. Brimacombe, R. (1991) *Biochimie*, **73**, 927-936.
31. Brockdorff, N., Ashworth, A., Kay, G.F., McCabe, V.M., Norris, D.P., Cooper, P.J., Swift, S. and Rastan, S. (1992) *Cell*, **71**, 515-526.
32. Yamada, M., Izu, H., Nitta, K., Kurihara, K. and Sakurai, T. (1998) *Biotechniques*, **25**, 72-75.
33. Ausubel, F.M., Brent, R., Kingston, R.E., Moore, D.D., Seidman, J.G., Smith, J.A. and Struhl, K. (1987) In Chanda, V. (ed.), *Current Protocols in Molecular Biology*, Vol. 1. John Wiley & Sons, New York, NY.
34. Riggs, A.D., Singer-Sam, J. and Pfeifer, G.P. (1998) In Gould, H. (ed.), *Chromatin: A Practical Approach*. Oxford University Press, Oxford, pp. 79-109.
35. Buettner, V.L., LeBon, J.M., Gao, C., Riggs, A.D. and Singer-Sam, J. (2000) *Nucleic Acids Res.*, **28**, e25.
36. Rhee, Y., Valentine, M.R. and Termini, J. (1995) *Nucleic Acids Res.*, **23**, 3275-3282.
37. Steinecke, P., Herget, T. and Schreier, P.H. (1992) *EMBO J.*, **11**, 1525-1530.
38. Knowles, B.B., Howe, C.C. and Aden, D.P. (1980) *Science*, **209**, 497-499.